Δ3-tubulin impairs mitotic spindle morphology and increases nuclear size in pancreatic cancer cells

Kenta Baba[1, 2], Kenichiro Uemura[1], Ryota Nakazato[2], Faryal Ijaz[2], Shinya Takahashi[1], Koji Ikegami[2*]

[1]Department of Surgery, Graduate School of Biomedical and Health Sciences, Hiroshima University, 1-2-3 Kasumi, Minami-ku, Hiroshima, 734-8553, Japan

[2]Department of Anatomy and Developmental Biology, Graduate School of Biomedical and Health Sciences, Hiroshima University, 1-2-3 Kasumi, Minami-ku, Hiroshima, 734-8553, Japan

Corresponding author: Koji Ikegami, PhD

Department of Anatomy and Developmental Biology, Graduate School of Biomedical and Health Sciences, Hiroshima University, 1-2-3 Kasumi, Minami-ku, Hiroshima, 734-8553 Japan

Telephone: +81-82-257-5110

E-mail: k-ikegami@hiroshima-u.ac.jp

Keywords: Δ3-tubulin; Post-translational modification; Microtubules; Spindle morphology; Mitosis; Pancreatic cancer

Abstract

Cancer cell proliferation is affected by post-translational modifications of tubulin. Especially, overexpression or depletion of enzymes for modifications on tubulin C-terminal region perturbs dynamic instability of spindle body. Those modifications include processing of C-terminal amino acids of α-tubulin; detyrosination, and a removal of penultimate glutamic acid (Δ2). We previously found a further removal of the third last glutamic acid, which generates so-called Δ3-tubulin. Effects of Δ3-tubulin on spindle integrities and cell proliferation remain to be elucidated. In this study, we investigated impacts of forced expression of Δ3-tubulin on the structure of spindle bodies and cell division in a pancreatic cancer cell line, PANC-1. Overexpression of HA-tagged Δ3-tubulin impaired the morphology and orientation of spindle bodies during cell division in PANC-1 cells. In particular, spindle bending was most significantly increased. Expression of EGFP-tagged Δ3-tubulin driven by the endogenous promoter of human *TUBA1B* also deformed and misoriented spindle bodies. Spindle bending and condensation defects were significantly observed by EGFP-Δ3-tubulin expression. Furthermore, EGFP-Δ3-tubulin expression increased the nuclear size in a dose-dependent manner of EGFP-Δ3-tubulin expression. Expression of EGFP-Δ3-tubulin tended to slow down cell proliferation. Taken together, our results demonstrate that Δ3-tubulin affects the spindle integrity and cell division.

Introduction

Cell division is crucial for the reproduction, growth, and regeneration of multicellular eukaryotes. The proper chromosome segregation is an important process of the cell division for daughter cells to inherit robustly genetic information from a parent cell. The chromosome segregation requires the spindle body which consists of microtubule-based spindle fibers and centrosome-based spindle poles and the surrounding asters. Impairments in the spindle bodies lead to aneuploidy, which is a risk factor for cancer and a variety of human diseases [1–3]. Meanwhile, defects of spindle bodies result in the failure of cell division and finally cause cell death [2]. Dynamic instability of microtubules is a key factor for the proper structure and function of spindle bodies. Both destabilization and over-stabilization of microtubules impair the morphology and function of spindle bodies. Thus, both microtubule-depolymerizing and microtubule-stabilizing agents, such as vinca alkaloids and paclitaxel, can work as anticancerous drugs [4].

The microtubule is bundles of polymerized heterodimers of α-tubulin and β-tubulin. The tubulin undergoes numerous post-translational modifications (PTMs) [5, 6]. Most of the PTMs are concentrated at the C-terminus of tubulin, which is exposed to the surface of microtubule. Some of these PTMs are reversible: detyrosination/re-tyrosination [7, 8], polyglutamylation/deglutamylation [9–11]. In contrast, sequential removals of amino acids from α-tubulin C-terminus are thought to be irreversible, except detyrosination where the last amino acid, tyrosine, is removed [8]. Further removal of the penultimate glutamic acid from the detyrosinated α-tubulin generates so-called Δ2-tubulin, which is thought to be an irreversible PTM [12]. Recently, we and another group have found that the removal of the third last glutamic acid from the Δ2-tubulin generates Δ3-tubulin *in vitro* and *in vivo* [13, 14].

The majority of tubulin PTMs are accumulated in long-lived, i.e. highly stable microtubules, such as those in neuronal processes, cilia, and flagella [5, 6]. Microtubules in

spindle bodies are reported to be enriched by some of those PTMs [5, 6]. Spindle fibers are strongly positive for detyrosinated [15], glutamylated [16] and acetylated tubulin [17]. Among them, detyrosinated tubulin has been shown to regulate chromosome alignment and spindle size during mitosis [18–20]. By contrast, tyrosinated astral microtubules are reported to be essential for spindle positioning [5, 21, 22]. Furthermore, centriolar microtubules have high levels of polyglutamylated tubulin, which has been associated with centriole maintenance and functions during mitosis [23, 24]. Δ2- and Δ3-tubulin have been also accumulated in long-lived stable microtubules; Δ2-tubulin is detected in centrioles [25, 26] in addition to brain neurons [14], but not Δ3-tubulin. It remains unclear whether Δ3-tubulin accumulation affects cell division or not.

Some PTMs of tubulin have been reported to be associated with cancer growth, metastasis, and anticancer drug resistance [27, 28]. Pancreatic ductal adenocarcinoma (PDAC) has a strong tendency to invade and metastasize and is one of the most intractable solid human cancers with an extremely poor prognosis [29, 30]. Recently, novel regimens and anticancer drugs for PDAC are expected to prolong life, but they have not significantly improved the prognosis [30–32]. This is partly because PDAC is a heterogeneous disease at the molecular and pathological level [29]. Several PTMs of tubulin have been reported to be associated with pancreatic cancer cells. In pancreatic cancer, tubulin tyrosine ligase-like family member 4 (TTLL4) and histone deacetylase 6 (HDAC6), tubulin-modifying enzymes, were suggested to promote cell proliferation [33, 34], and a tubulin isotype β3-tubulin was associated with anticancer drug resistance, tumor development, and metastatic ability [35, 36]. The association between Δ3-tubulin and pancreatic cancer and effects of Δ3-tubulin on PDAC cells are not investigated.

In this study, we examined whether the expression of Δ3-tubulin affects cell division, proliferation, and nuclear size. To this end, we used not only the transient overexpression but also the endogenous *TUBAB1* promoter-driven steady expression of Δ3-tubulin by using a

genome editing technique, which we developed recently [37], against a PDAC cell line, PANC-1. We found that Δ3-tubulin impairs the mitotic spindle morphology, tends to slow down cell proliferation, and increases nuclear size in PANC-1 cells.

Materials and methods

Cell culture and transfection

The human pancreatic cancer PANC-1 cell line was purchased from RIKEN Bioresources Cell Bank (Ibaraki, Japan), and routinely grown in RPMI-1640 (Wako; Osaka, Japan) supplemented with 10% fetal bovine serum (FBS) at 37ºC in a humidified atmosphere containing 5% CO_2. Cells were seeded on 60-mm dish, glass slip, or plastic coverslips (Cell Desk LF1; Sumitomo Bakelite, Tokyo, Japan). For cell number count, cells were harvested from dishes with trypsin, and the actual number of cells was counted using a hemocytometer. Polyethylenimine (PEI) was used for transfection [38]. Transfection complexes were prepared by mixing PEI and DNA at a ratio of 3:1 in weight.

Generation of stable cell lines

Stable cell lines with knock-in of labeled proteins into 5'UTR were generated as reported previously [37]. The sgRNA-targeting sequence with PAM (underline), CCTCGACTCTTAGCTTGTCG<u>GGG</u>, for *TUBA1B* 5'UTR was selected with Broad Institutes GPP sgRNA Designer. The 20-bp target sequence was sub-cloned into CMV-Cas9-2A-GFP plasmid backbone (ATUM, Newark, CA, USA). Cells were co-transfected with Cas9/gRNA-expression plasmids and donor plasmids selected with 1.5 mg/mL G418, and subjected to flow cytometry.

Antibodies

The following antibodies were used for immunofluorescence (IF) and/or western blotting (WB) at each dilutions: HA-tag (1:1000 for IF, rabbit mAb C29F4, Cell Signaling; 1:4000 for WB, mouse mAb 16B12, Biolegend), α-tubulin (1:5000 for IF and WB, mouse mAb DM1A, Sigma), GFP (1:2000 for IF, rabbit pAb, ab6556, Abcam; 1:1000 for WB, rabbit pAb, #598, MBL), Alexa fluorophore-conjugated secondary antibodies (1:500 for IF, Thermo), and horseradish peroxidase-conjugated secondary antibodies (1:10000 for WB, Jackson Immuno Research Laboratories). Anti-Δ3-tubulin (1:2000 for IF, rabbit pAb) was generated against a peptide CVEGEGEEEG, and affinity-purified with the antigen peptide after adsorbing anti-Δ2 fractions with CVEGEGEEEGE peptides (Sigma-Aldrich Japan, Tokyo, Japan).

Immunofluorescence microscopy

Cells were fixed with 4% paraformaldehyde (PFA, pH 7.5) for 20 min at 37 ºC. Cells were blocked and permeabilized with 5% normal goat serum containing 0.1% Triton X-100 in PBS for 1 h at room temperature. Then, cells were incubated at 4ºC with primary antibodies diluted in the blocking solution overnight, and stained with Alexa Fluor-conjugated secondary antibodies and DAPI (1 μg/ml, DOJINDO; Kumamoto, Japan) for 1 h. Samples were mounted on glass slides with VECTASHIELD mounting medium (Vector Laboratories, Burlingame, CA, USA). Fluorescence images were obtained with a laser scanning confocal microscope (FV1000-D, Olympus; Tokyo, Japan) equipped with a 60×, N.A. 1.35 objective lens. GFP-positive cells and DAPI-stained nuclei were counted using tools of ImageJ (https://imagej.nih.gov/ij/). Fluorescence intensities were measured using the ‘‘Oval’’ tool of ImageJ. Nuclear areas were measured using the “analyze particles” tool of ImageJ. GFP intensity was measured at three regions in cytoplasm per cell. Cells with average cytoplasmic GFP intensity ≥ 120 were classified as EGFP-positive group. The cut-off value, 120, was

determined with the averaged background signal intensities in untransfected cell cytoplasm.

Western blot analyses

Cell lysates were harvested by adding 1x SDS-PAGE sample buffer to the confluent cells and heated at 95ºC for 10 minutes and loaded on to an acrylamide gel. Following protein transfer, PVDF membranes (Merk Millipore, Burlington, MA, USA) were blocked with 5% BSA/TBST for 1 h at room temperature. Primary antibodies diluted in 1% BSA/TBST were added, and the membranes were incubated at 4ºC overnight. The membranes were incubated with HRP-conjugated secondary antibodies for 1 h. The signals were developed using ECL prime (GE Healthcare, Chicago, IL, USA) and detected with VersaDoc 5000 (Bio-Rad, Hercules, CA, USA).

Statistical analysis

The statistical significance of the difference between two means was determined using a two-tailed unpaired Student's t-test. The categorical data were compared using a chi-squared test. Differences were considered significant when $P < 0.05$. All statistical calculations were carried out using JMP statistical software, version 16.0 (SAS Institute, Cary, NC, USA).

Results

Overexpression of Δ3-tubulin impairs mitotic spindle morphology in PANC-1 cells

To investigate the effects of Δ3-tubulin in PANC-1 cells, we first transiently overexpressed HA-tagged Δ3-tubulin in the PANC-1 cell line where the expression was driven by the PGK promoter. PGK promoter was chosen to prevent putative toxic effects by commonly used strong CMV promoter and enhancer. When the CMV promoter was used, many cells

showed strange shapes due to highly unbalanced expression of α- and β-tubulin and few GFP-positive mitotic cells were observed. The expression of HA-Δ3-tubulin was confirmed with anti-Δ3-tubulin polyclonal antibodies. Cells detected with an anti-HA antibody were positive for anti-Δ3-tubulin immunoreactivities in the HA-Δ3-tubulin-expresssing cells (Fig. 1A, right). Neither plane HA-α-tubulin-expressing or non-transfected cells were stained with anti-Δ3-tubulin antibodies (Fig. 1A, left and middle).

We then examined the morphology of mitotic spindles in the PANC-1 cells that expressed HA-Δ3-tubulin or unmodified HA-α-tubulin using confocal microscopy. The morphology of mitotic spindles were classified into seven phenotypes (Fig. 1B), according to the work by Goshima and his colleagues [39]. HA-Δ3-tubulin overexpression caused increase in the rate of abnormal spindle morphologies compared to plane HA-α-tubulin overexpression (Fig. 1C; 68% versus 45%, $p = 0.0314$). Among the six abnormal spindle morphologies, the spindle bending was significantly increased in HA-Δ3-tubulin-overexpressing PANC-1 cells (Fig. 1C; 18% versus 5%, $p = 0.0439$). The short spindle and spindle misalign showed tendencies of increase in the HA-Δ3-tubulin-overexpressing PANC-1 cells, though statistical values were not less than 0.05 (Fig. 1C; short spindle: 5% versus 0%, $p = 0.1526$; spindle misalign: 32% versus 18%, $p = 0.1396$). These results indicate that the overexpression of Δ3-tubulin impairs mitotic spindle morphology in PANC-1 cells.

Steady expression of Δ3-tubulin at the physiological level impairs mitotic spindle morphology

To avoid toxic effects by overexpression of exogenous proteins, we next attempted to use cell lines that steadily expressed tagged tubulin under the endogenous α-tubulin promoter. To this end, we established PANC-1 cells that expressed Δ3-tubulin fused with the fluorescent protein EGFP by CRISPR/Cas9-mediated genome editing against the 5'UTR of α-tubulin [37]

(Fig. 2A). To keep the heterogeneity of cells, we did not clone knock-in cells, and simply collected EGFP-positive cells with FACS. The expression of EGFP-fused α-tubulin was confirmed by detecting a ~75-kDa band with anti-GFP antibodies in western blotting (Fig. 2B; arrowhead). The expression of EGFP-fused Δ3-tubulin was further verified with anti-Δ3-tubulin antibodies in immunocytochemistry (Fig. 2C).

We then examined the morphology of the spindle during cell division using confocal microscopy as done in experiments with HA-α-tubulin overexpression. We here also classified the morphology of spindles into seven types as shown in figure 2D. Steady expression of EGFP-α-tubulin under the endogenous α-tubulin promoter seemed to be less toxic than overexpression of HA-α-tubulin with the exogenous PGK promoter as the rate of abnormal spindle shapes was lower in cells steadily expressing EGFP-α-tubulin than in cells overexpressing HA-α-tubulin (35% versus 45%) (Fig. 1C and 2E).

Steady expression of EGFP-Δ3-tubulin at the physiological level caused the significant increase in the rate of abnormal spindles, compared to that of plane EGFP-α-tubulin (Fig. 2E; 54% versus 35%, $p = 0.0028$). Among the abnormal spindles, two types of morphologies were significantly increased in EGFP-Δ3-tubulin-expressing PANC-1 cells compared to EGFP-α-tubulin-expressing cells. The occurrence rate of spindle bending was 6.7% in EGFP-Δ3-tubulin-expressing cells against 0% in EGFP-α-tubulin-expressing cells ($p = 0.0040$) (Fig. 2E). The condensation defect was increased in Δ3-tubulin-expressing cells compared to plane α-tubulin-expressing cells (Fig. 2D; 3.3% versus 0%, $p = 0.0437$). In addition, the occurrence rate of misalign tended to be higher in EGFP-Δ3-tubulin-expressing cells than in EGFP-α-tubulin-expressing cells (Fig. 2E; 16.7% versus 10%, $p = 0.1287$). These results indicate that steady expression of Δ3-tubulin at the physiological level impairs the mitotic spindle morphology in PANC-1 cells.

Steady expression of Δ3-tubulin at the physiological level tends to slow down cell proliferation of PANC-1 cells

Next, to evaluate impacts of Δ3-tubulin expression on cell proliferation in PANC-1 cells, we compared the number of cells between EGFP-Δ3-tubulin- and EGFP-α-tubulin-expressing cells. In this experiment, we also did not perform cloning of knock-in cells to keep the heterogeneity of cells so that we were able to behaviors of cell population (Fig. 3A). We measured the actual number of cells on the culture dish at 48 h and 96 h after seeding the cells at 7.0×10^3 cells/cm^2. EGFP-Δ3-tubulin-expressing PANC-1 cells showed slight tendency of slower proliferation than EGFP-α-tubulin-expressing cells at both 48 h ($12.9 \times 10^3 \pm 0.9 \times 10^3$ cells/cm^2 versus $14.2 \times 10^3 \pm 0.8 \times 10^3$ cells/cm^2, $p = 0.0676$) and 96 h ($47.8 \times 10^3 \pm 2.7 \times 10^3$ cells/cm^2 versus $50.8 \times 10^3 \pm 2.2 \times 10^3$ cells/cm^2, $p = 0.1249$) (Fig. 3B). No decrease in cell proliferation of EGFP-tubulin-expressing cells compared to plane wildtype cells indicates again that the steady expression of EGFP-α-tubulin under the endogenous promoter per se has almost no toxicity to cells and thus little impairs cell proliferation (Fig. 3B). Together, these results suggest that the expression of Δ3-tubulin could slow down cell proliferation in PANC-1 cells.

Steady expression of Δ3-tubulin at the physiological level increases the size of nucleus of PANC-1 cells in a dose-dependent manner

We finally investigated the impact of Δ3-tubulin expression on the size of nuclei, since the expression of Δ3-tubulin impairs the spindle morphology (Fig. 1, 2). EGFP-Δ3-tubulin-expressing cells had enlarged nuclei more frequently than EGFP-α-tubulin-expressing cells (Fig. 4A; arrowheads). The quantified data supported the observation of fluorescence microscopy. To this end, we measured the maximum nuclear cross-sectional area using PANC-1 cells that were heterogeneous population of EGFP-Δ3-tubulin- or EGFP-α-tubulin-expressing cells. The maximum nuclear cross-sectional area was significantly increased in GFP-positive

cells of EGFP-Δ3-tubulin-experssing cells than in those of EGFP-α-tubulin-expressing cells (Fig. 4B right; 250.7 ± 84.2 μm^2 versus 222.1 ± 74.7 μm^2, $p = 0.0005$). These increases were not detected between EGFP-Δ3-tubulin- and EGFP-α-tubulin-expressing cells when the maximum nuclear cross-sectional area was compared in cells with dim or no EGFP signals (Fig. 4B left; 221.2 ± 78.1 μm^2 versus 234.8 ± 81.4 μm^2, $p = 0.2899$). Among the EGFP-positive cells, the maximum nuclear cross-sectional area was positively correlated with the intensity of EGFP fluorescence in EGFP-Δ3-tubulin-expressing cells (Fig. 4C: $p < 0.0001$, r = 0.320). In contrast, such positive correlation was not observed in EGFP-α-tubulin-expressing cells (Fig. 4C; $p = 0.6662$). These results thus indicate that the expression of Δ3-tubulin increases the nuclear size in PANC-1 cells in a dose-dependent manner.

Discussion

In this study, we demonstrated that the expression of Δ3-tubulin impairs mitotic spindle morphology and tends to inhibit cell proliferation. We also found that Δ3-tubulin increased nuclear size in a dose-dependent manner.

We have shown that both transient and steady overexpression of Δ3-tubulin in PANC-1 cells impaired mitotic spindle morphology (Fig. 1, 2). Spindle microtubules are particularly enriched by detyrosination and acetylation among tubulin PTMs [15, 17], and these modifications have been reported to be associated with regulation of chromosome segregation as well as the spindle morphology and function [18–20, 40]. These previous studies describe that detyrosination is involved in the proper chromosome alignment and mitotic error correction [18–20], and that deletion of the tubulin acetylase ATAT1 causes formation of monopolar spindles [40]. It has also been reported that the expression of an α-tubulin subtype that has less acidic C-terminal tail results in the displacement of the spindle [41]. It is plausible that the misalignment of spindles caused by the expression of Δ3-tubulin could occur through similar

mechanisms since Δ3-tubulin lacks two negatively charged glutamates from the α-tubulin tail. In contrast, morphological abnormalities such as spindle bending and condensation defect, which were observed in this study, have not been reported to be related to manipulation of tubulin PTMs so far, and might be specific to Δ3-tubulin. Interestingly, artificially expressed Δ3-tubulin was accumulated around spindle poles only in these two unique defects, while it was distributed throughout spindle fibers in other types of defects (Fig. 2D). The accumulation of Δ3-tubulin could underlie the spindle bending and condensation defects. The molecular mechanism will be studied in the future work.

The expression of Δ3-tubulin showed an inhibitory tendency toward cell proliferation (Fig. 3). Earlier studies on tubulin PTMs have shown that reduction of detyrosination delays mitotic progression and that deletion of the tubulin acetyltransferase ATAT1 prolongs the pre-mitotic period [18, 20, 40]. Given that Δ3-tubulin is thought to be irreversible [13, 14], expression of Δ3-tubulin could result in the decrease of relative amount of detyrosinated tubulin in spindle. It is plausible that the expression of Δ3-tubulin is associated with the slowdown of cell proliferation, which is caused by impaired or delayed cell division due to abnormal spindle morphology as observed in the decrease of detyrosination and acetylation.

The stable expression of Δ3-tubulin increased the maximum nuclear cross-sectional area in an EGFP-Δ3-tubulin dose-dependent manner (Fig. 4). A simple explanation of the phenomenon is the occurrence of increase in DNA amount caused by polyploidy abnormality, which is often observed in spindle deficiencies [1–3]. Another possibility could be plausible that the abnormal tubulin PTMs affects nuclear morphology directly. A recent study has reported that dysregulated tubulin C-terminal PTMs result in abnormal nuclear morphology; decrease in tubulin glutamylation causes multinucleation [42]. Since Δ3-tubulin lacks two negatively charged glutamate residues, the abnormality of nuclear shape is a common result of decrease in the negative charges from tubulin C-terminus.

In conclusion, we demonstrate in this work that Δ3-tubulin causes mitotic spindle morphology abnormalities, a tendency to slow down cell proliferation, and an increase in nuclear size. As Δ3-tubulin formation is an irreversible reaction [13, 14], it can accumulate in excess on spindle microtubules. The relationship between abnormal accumulation of post-translational modifications and diseases has been reported [5, 6]. Our findings could offer a concept of the relationship between abnormal accumulation of Δ3-tubulin and diseases, at least, in terms of abnormal chromosome distribution.

References

1. Bakhoum SF, Cantley LC (2018) The Multifaceted Role of Chromosomal Instability in Cancer and Its Microenvironment. Cell 174:1347–1360
2. Vitale I, Galluzzi L, Castedo M, Kroemer G (2011) Mitotic catastrophe: a mechanism for avoiding genomic instability. Nat Rev Mol Cell Biol 12:385–392
3. Hanahan D, Weinberg RA (2011) Hallmarks of cancer: The next generation. Cell 144:646–674
4. Kavallaris M (2010) Microtubules and resistance to tubulin-binding agents. Nat Rev Cancer 10:194–204
5. Janke C, Magiera MM (2020) The tubulin code and its role in controlling microtubule properties and functions. Nat Rev Mol Cell Biol 21:307–326
6. Ikegami K, Setou M (2010) Unique post-translational modifications in specialized microtubule architecture. Cell Struct. Funct. 35:15–22
7. Barra HS, Arce CA, Rodríguez JA, Caputto R (1974) Some common properties of the protein that incorporates tyrosine as a single unit and the microtubule proteins. Biochem Biophys Res Commun 60:1384–1390
8. Argaraña CE, Barra HS, Caputto R (1978) Release of [14C]tyrosine from tubulinyl-[14C]tyrosine by brain extract. Separation of a carboxypeptidase from tubulin-tyrosine ligase. Mol Cell Biochem 19:17–21
9. Eddé B, Rossier J, Le Caer JP, Desbruyères E, Gros F, Denoulet P (1990) Posttranslational glutamylation of α-tubulin. Science 247:83–85
10. Kimura Y, Kurabe N, Ikegami K, Tsutsumi K, Konishi Y, Kaplan OI, Kunitomo H, Iino Y, Blacque OE, Setou M (2010) Identification of tubulin deglutamylase among Caenorhabditis elegans and mammalian cytosolic carboxypeptidases (CCPs). J Biol Chem 285:22936–22941

11. Rogowski K, van Dijk J, Magiera MM, Bosc C, Deloulme JC, Bosson A, Peris L, Gold ND, Lacroix B, Bosch Grau M, Bec N, Larroque C, Desagher S, Holzer M, Andrieux A, Moutin MJ, Janke C (2010) A family of protein-deglutamylating enzymes associated with neurodegeneration. Cell 143:564–578

12. Paturle-Lafanechère L, Eddé B, Denoulet P, Van Dorsselaer A, Mazarguil H, Le Caer JP, Wehland J, Job D (1991) Characterization of a Major Brain Tubulin Variant Which Cannot Be Tyrosinated. Biochemistry 30:10523–10528

13. Berezniuk I, Vu HT, Lyons PJ, Sironi JJ, Xiao H, Burd B, Setou M, Angeletti RH, Ikegami K, Fricker LD (2012) Cytosolic carboxypeptidase 1 is involved in processing α- and β-tubulin. J Biol Chem 287:6503–6517

14. Aillaud C, Bosc C, Saoudi Y, Denarier E, Peris L, Sago L, Taulet N, Cieren A, Tort O, Magiera MM, Janke C, Redeker V, Andrieux A, Moutin MJ (2016) Evidence for new C-terminally truncated variants of α-and β-tubulins. Mol Biol Cell 27:640–653

15. Gundersen GG, Bulinski JC (1986) Distribution of tyrosinated and nontyrosinated α-tubulin during mitosis. J Cell Biol 102:1118–1126

16. Lacroix B, van Dijk J, Gold ND, Guizetti J, Aldrian-Herrada G, Rogowski K, Gerlich DW, Janke C (2010) Tubulin polyglutamylation stimulates spastin-mediated microtubule severing. J Cell Biol 189:945–954

17. Piperno G, LeDizet M, Chang XJ (1987) Microtubules containing acetylated alpha-tubulin in mammalian cells in culture. J Cell Biol 104:289–302

18. Barisic M, Silva e Sousa R, Tripathy SK, Magiera MM, Zaytsev AV, Pereira AL, Janke C, Grishchuk EL, Maiato H (2015) Microtubule detyrosination guides chromosomes during mitosis. Science 348:799–803

19. Ferreira LT, Orr B, Rajendraprasad G, Pereira AJ, Lemos C, Lima JT, Guasch Boldú C, Ferreira JG, Barisic M, Maiato H (2020) α-Tubulin detyrosination impairs mitotic

error correction by suppressing MCAK centromeric activity. J Cell Biol 219:e201910064

20. Liao S, Rajendraprasad G, Wang N, Eibes S, Gao J, Yu H, Wu G, Tu X, Huang H, Barisic M, Xu C (2019) Molecular basis of vasohibins-mediated detyrosination and its impact on spindle function and mitosis. Cell Res 29:533–547

21. Noatynska A, Gotta M, Meraldi P (2012) Mitotic spindle (DIS)orientation and DISease: Cause or consequence? J. Cell Biol. 199:1025–1035

22. Godin JD, Colombo K, Molina-Calavita M, Keryer G, Zala D, Charrin BC, Dietrich P, Volvert ML, Guillemot F, Dragatsis I, Bellaiche Y, Saudou F, Nguyen L, Humbert S (2010) Huntingtin Is Required for Mitotic Spindle Orientation and Mammalian Neurogenesis. Neuron 67:392–406

23. Bobinnec Y, Khodjakov A, Mir LM, Rieder CL, Eddé B, Bornens M (1998) Centriole disassembly in vivo and its effect on centrosome structure and function in vertebrate cells. J Cell Biol 143:1575–1589

24. Abal M, Keryer G, Bornens M (2005) Centrioles resist forces applied on centrosomes during G2/M transition. Biol Cell 97:425–434

25. Paturle-Lafanechère L, Manier M, Trigault N, Pirollet F, Mazarguil H, Job D (1994) Accumulation of delta 2-tubulin, a major tubulin variant that cannot be tyrosinated, in neuronal tissues and in stable microtubule assemblies. J Cell Sci 107:1529–1543

26. Smertenko A, Blume Y, Viklický V, Opatrný Z, Dráber P (1997) Post-translational modifications and multiple tubulin isoforms in Nicotiana tabacum L. cells. Planta 201:349–358

27. Banerjee A (2002) Increased levels of tyrosinated α-, βIII-, and βIV-tubulin isotypes in paclitaxel-resistant MCF-7 breast cancer cells. Biochem Biophys Res Commun 293:598–601

28. Mialhe A, Lafanechère L, Treilleux I, Peloux N, Dumontet C, Brémond A, Panh MH, Payan R, Wehland J, Margolis RL, Job D (2001) Tubulin detyrosination is a frequent occurrence in breast cancers of poor prognosis. Cancer Res 61:5024–5027

29. Vincent A, Herman J, Schulick R, Hruban RH, Goggins M (2011) Pancreatic cancer. The Lancet 378:607–620

30. Sung H, Ferlay J, Siegel RL, Laversanne M, Soerjomataram I, Jemal A, Bray F (2021) Global Cancer Statistics 2020: GLOBOCAN Estimates of Incidence and Mortality Worldwide for 36 Cancers in 185 Countries. CA Cancer J Clin 71:209–249

31. Siegel RL, Miller KD, Jemal A (2020) Cancer statistics, 2020. CA Cancer J Clin 70:7–30

32. Murakami Y, Uemura K, Hashimoto Y, Kondo N, Nakagawa N, Takahashi S, Shintakuya R, Sueda T (2016) Survival effects of adjuvant gemcitabine plus S-1 chemotherapy on pancreatic carcinoma stratified by preoperative resectability status. J Surg Oncol 113:405–412

33. Kashiwaya K, Nakagawa H, Hosokawa M, Mochizuki Y, Ueda K, Piao L, Chung S, Hamamoto R, Eguchi H, Ohigashi H, Ishikawa O, Janke C, Shinomura Y, Nakamura Y (2010) Involvement of the tubulin tyrosine ligase-like family member 4 polyglutamylase in PELP1 polyglutamylation and chromatin remodeling in pancreatic cancer cells. Cancer Res 70:4024–4033

34. Li D, Sun X, Zhang L, Yan B, Xie S, Liu R, Liu M, Zhou J (2014) Histone deacetylase 6 and cytoplasmic linker protein 170 function together to regulate the motility of pancreatic cancer cells. Protein Cell 5:214–223

35. Lee KM, Cao D, Itami A, Pour PM, Hruban RH, Maitra A, Ouellette MM (2007) Class III β-tubulin, a marker of resistance to paclitaxel, is overexpressed in pancreatic ductal adenocarcinoma and intraepithelial neoplasia. Histopathology 51:539–546

36. McCarroll JA, Sharbeen G, Liu J, Youkhana J, Goldstein D, McCarthy N, Limbri LF, Dischl D, Ceyhan GO, Erkan M, Johns AL, Biankin AV, Kavallaris M, Phillips PA (2015) βIII-Tubulin: A novel mediator of chemoresistance and metastases in pancreatic cancer. Oncotarget 6:2235–2249

37. Ijaz F, Ikegami K (2021) Knock-in of labeled proteins into 5'utr enables highly efficient generation of stable cell lines. Cell Struct Funct 46:21–35

38. Longo PA, Kavran JM, Kim MS, Leahy DJ (2013) Transient mammalian cell transfection with polyethylenimine (PEI). Methods Enzymol 529:227–240

39. Goshima G, Wollman R, Goodwin SS, Zhang N, Scholey JM, Vale RD, Stuurman N (2007) Genes required for mitotic spindle assembly in Drosophila S2 cells. Science 316:417–421

40. Rasamizafy SF, Delsert C, Rabeharivelo G, Cau J, Morin N, van Dijk J (2021) Mitotic acetylation of microtubules promotes centrosomal plk1 recruitment and is required to maintain bipolar spindle homeostasis. Cells 10:1859

41. Denarier E, Ecklund KH, Berthier G, Favier A, O'Toole ET, Gory-Fauré S, de Macedo L, Delphin C, Andrieux A, Markus SM, Boscheron C (2021) Modeling a disease-correlated tubulin mutation in budding yeast reveals insight into MAP-mediated dynein function. Mol Biol Cell 32:ar10

42. Wang L, Paudyal SC, Kang Y, Owa M, Liang FX, Spektor A, Knaut H, Sánchez I, Dynlacht BD (2022) Regulators of tubulin polyglutamylation control nuclear shape and cilium disassembly by balancing microtubule and actin assembly. Cell Res 32:190–209

Acknowledgements

We thank M. Hamada and Y. Hayashi for technical assistances. This work was supported in part by JSPS Grants-in-Aids for Scientific Research (C) (22K08776) to K.U. and K.I., and by the Uehara Memorial Foundation (to K.I.). A part of this work was the result of using research equipment shared in the Analysis Center of Life Science, Natural Science Center for Basic Research and Development, Hiroshima University, and the Research Institute for Radiation Biology and Medicine, Hiroshima University (NBARD-00002) and the MEXT Project to promote public utilization of advanced research infrastructure (Program for supporting construction of core facilities; Grant Number JPMXS0441300023).

Author contributions

K.B., F.I., and K.I. designed the research; K.B., F.I., and R.N. carried out the experiments; K.B., R.N. and K.I. analyzed the data; K.U. and S.T. organized the collaboration; and K.B. and K.I. wrote the paper. All authors reviewed the manuscript.

Competing interests

The authors declare that they have no conflicts of interest.

Figure Legends

Fig. 1 Transient overexpression of Δ3-tubulin impairs mitotic spindle morphology in PANC-1 cells. **(A)** Representative immunocytochemical images showing Δ3-tubulin (green), HA-tubulin (red), and the nucleus (blue). Scale bar, 20 μm. **(B)** Classification of seven types of spindle morphologies. Top: representative immunocytochemical images with HA-tubulin (green), α-tubulin (red) and the nucleus (blue) stained. Scale bar, 20 μm. Bottom: schematic cartoons. **(C)** Quantified data of mitotic spindle morphologies (n = 44 from 5 independent experiments). Statistical analysis performed using the chi-squared test, and $p < 0.05$ was defined as statistically significant

Fig. 2 Steady expression of Δ3-tubulin at the physiological level impairs mitotic spindle morphology in PANC-1 cells. **(A)** Scheme of EGFP-tagged α-tubulin knock-in into 5'UTR of the human *TUBA1B*. The gRNA-5'UTR target sequence (magenta) upstream of the protospacer adjacent motif (PAM) (orange) in the 5'UTR are indicated. Neo^R, neomycin resistance gene cassette. **(B)** Western blot analyses of EGFP-α-tubulin and EGFP-Δ3-tubulin. The arrowhead indicates the band of EGFP-α-tubulin. **(C)** Representative immunocytochemical images showing Δ3-tubulin (red), EGFP-tubulin (green), and the nucleus (blue). Scale bar, 20 μm. **(D)** Representative immunocytochemical images showing seven types of spindle morphologies with EGFP-tubulin (green), α-tubulin (red) and the nucleus (blue) stained. Scale bar, 20 μm. **(E)** Quantified data of mitotic spindle morphologies (n = 120 from 6 independent experiments). Statistical analysis performed using the chi-squared test, and $p < 0.05$ was defined as statistically significant

Fig. 3 Steady expression of Δ3-tubulin at the physiological level tends to slow down cell

proliferation of PANC-1 cells. **(A)** Experimental scheme of the cell proliferation assay. Knock-in cells were double-selected with G418 and flow cytometry. **(B)** Quantified data of cell proliferation. The number of counted cells at 0, 48, and 96 h after seeding is plotted as mean ± SD from five independent experiments. Each experiment was performed in duplicate per condition. Statistical analysis performed using the two-tailed unpaired Student's t-test, and $p < 0.05$ was defined as statistically significant

Fig. 4 Steady expression of Δ3-tubulin at the physiological level increases the size of nucleus of PANC-1 cells in a dose-dependent manner. **(A)** Representative immunocytochemical images showing the nucleus (blue) and EGFP-tubulin (green). Arrowheads highlight large nuclei. Scale bar, 20 μm. **(B)** Quantified data of the maximum nuclear cross-sectional area. The data are plotted as mean ± SD from five independent experiments. GFP-negative group: $n = 256$ for wild type, $n = 56$ for EGFP-α-tubulin, $n = 69$ for EGFP-Δ3-tubulin. GFP-positive group: $n = 190$ for EGFP-α-tubulin, $n = 200$ for EGFP-Δ3-tubulin. **(C)** Correlation between the GFP intensity and the maximum nuclear cross-sectional area in GFP-positive group. Statistical analysis performed using two-tailed unpaired Student's t-test or correlation analysis, and $p < 0.05$ was defined as statistically significant

Figure 1

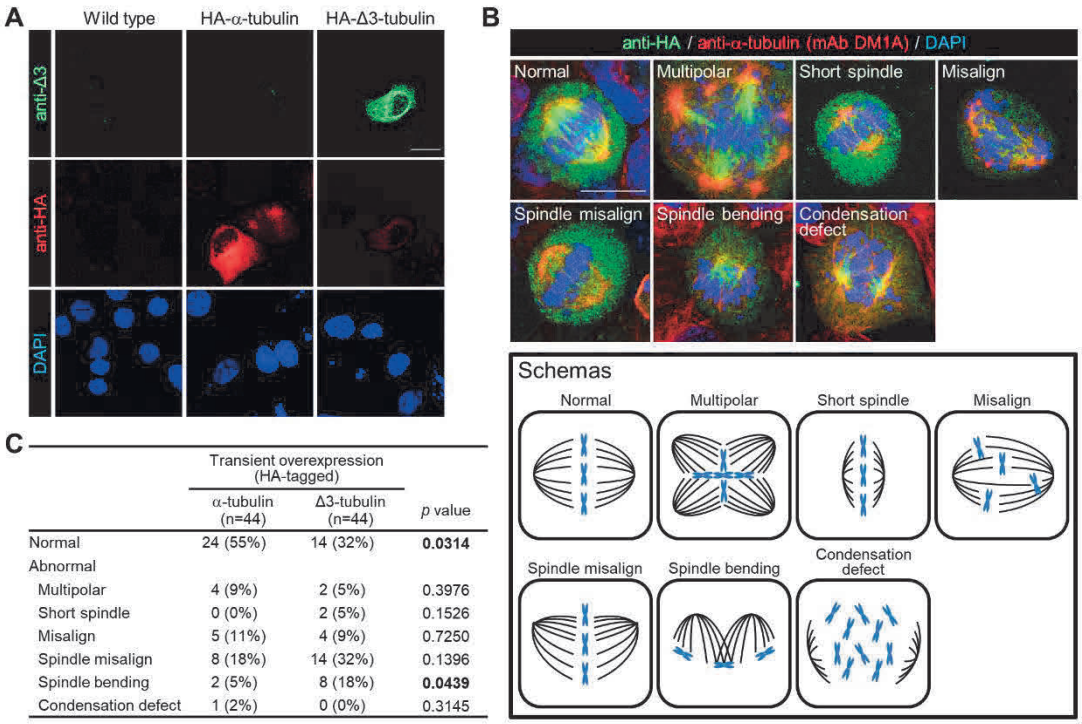

C

	Transient overexpression (HA-tagged)		
	α-tubulin (n=44)	Δ3-tubulin (n=44)	*p* value
Normal	24 (55%)	14 (32%)	**0.0314**
Abnormal			
Multipolar	4 (9%)	2 (5%)	0.3976
Short spindle	0 (0%)	2 (5%)	0.1526
Misalign	5 (11%)	4 (9%)	0.7250
Spindle misalign	8 (18%)	14 (32%)	0.1396
Spindle bending	2 (5%)	8 (18%)	**0.0439**
Condensation defect	1 (2%)	0 (0%)	0.3145

Figure 2

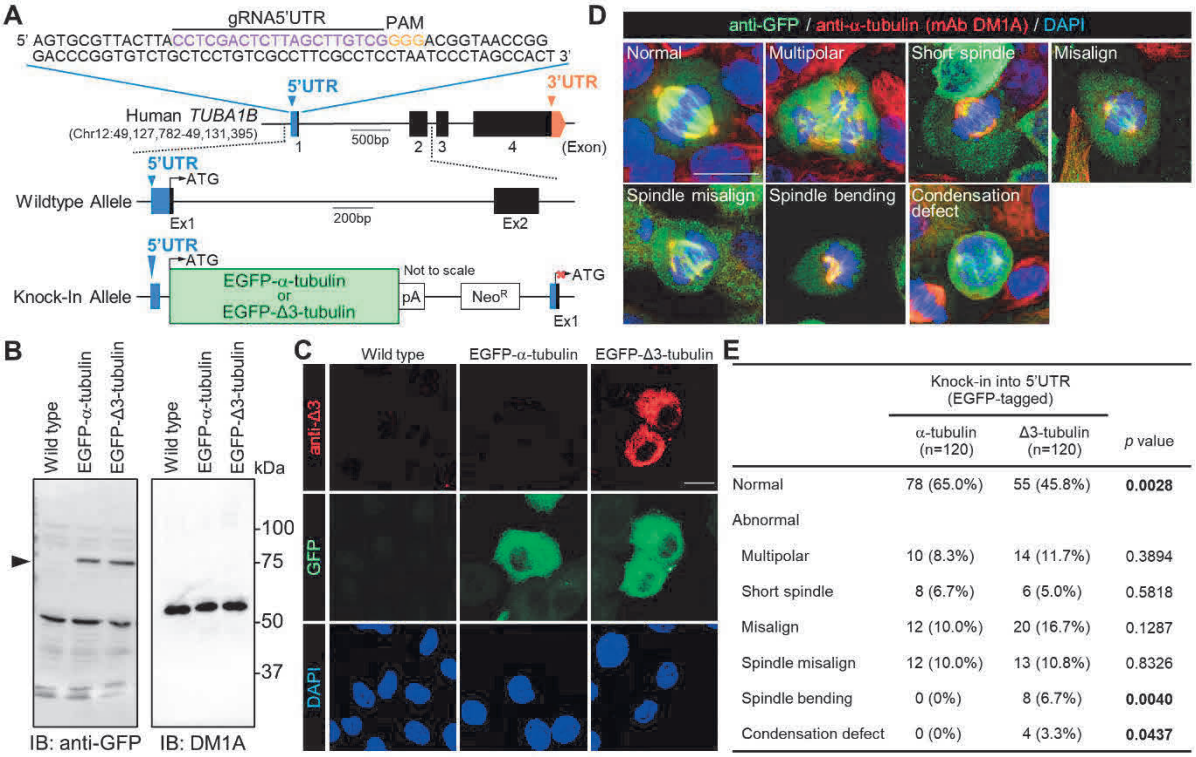

E

	Knock-in into 5'UTR (EGFP-tagged)		
	α-tubulin (n=120)	Δ3-tubulin (n=120)	*p* value
Normal	78 (65.0%)	55 (45.8%)	**0.0028**
Abnormal			
Multipolar	10 (8.3%)	14 (11.7%)	0.3894
Short spindle	8 (6.7%)	6 (5.0%)	0.5818
Misalign	12 (10.0%)	20 (16.7%)	0.1287
Spindle misalign	12 (10.0%)	13 (10.8%)	0.8326
Spindle bending	0 (0%)	8 (6.7%)	**0.0040**
Condensation defect	0 (0%)	4 (3.3%)	**0.0437**

Figure 3

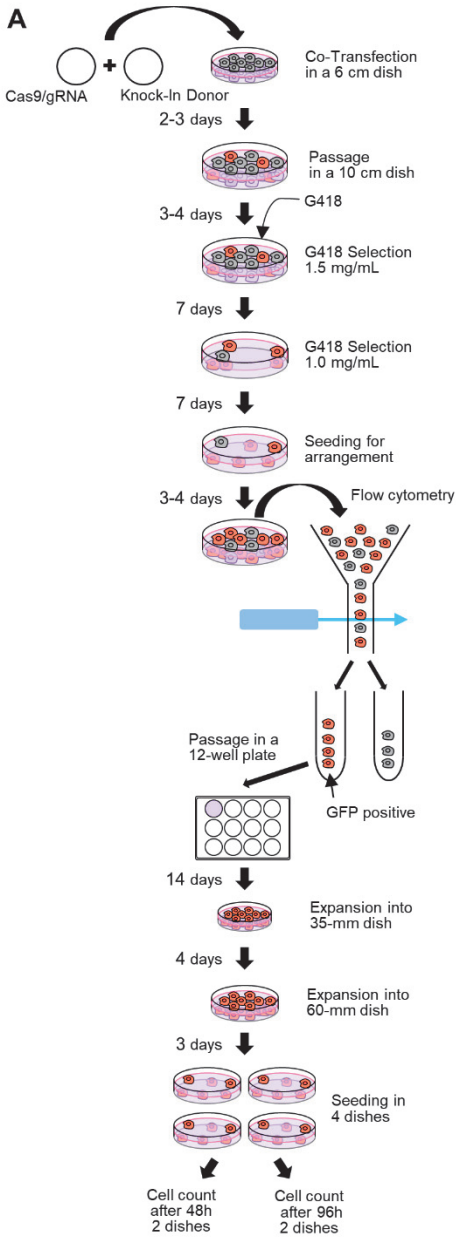
A
Cas9/gRNA
Knock-In Donor
Co-Transfection
in a 6 cm dish
2-3 days
Passage
in a 10 cm dish
3-4 days
G418
G418 Selection
1.5 mg/mL
7 days
G418 Selection
1.0 mg/mL
7 days
Seeding for
arrangement
3-4 days
Flow cytometry
Passage in a
12-well plate
GFP positive
14 days
Expansion into
35-mm dish
4 days
Expansion into
60-mm dish
3 days
Seeding in
4 dishes
Cell count
after 48h
2 dishes
Cell count
after 96h
2 dishes

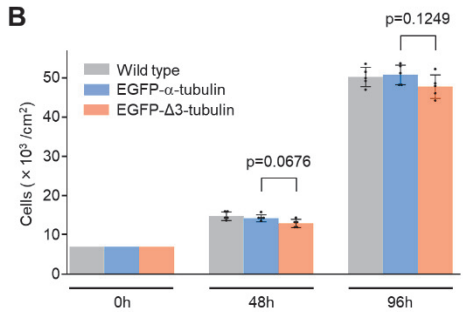
B
Wild type
EGFP-α-tubulin
EGFP-Δ3-tubulin
Cells (× 10³ /cm²)
0
10
20
30
40
50
p=0.0676
p=0.1249
0h
48h
96h

Figure 4

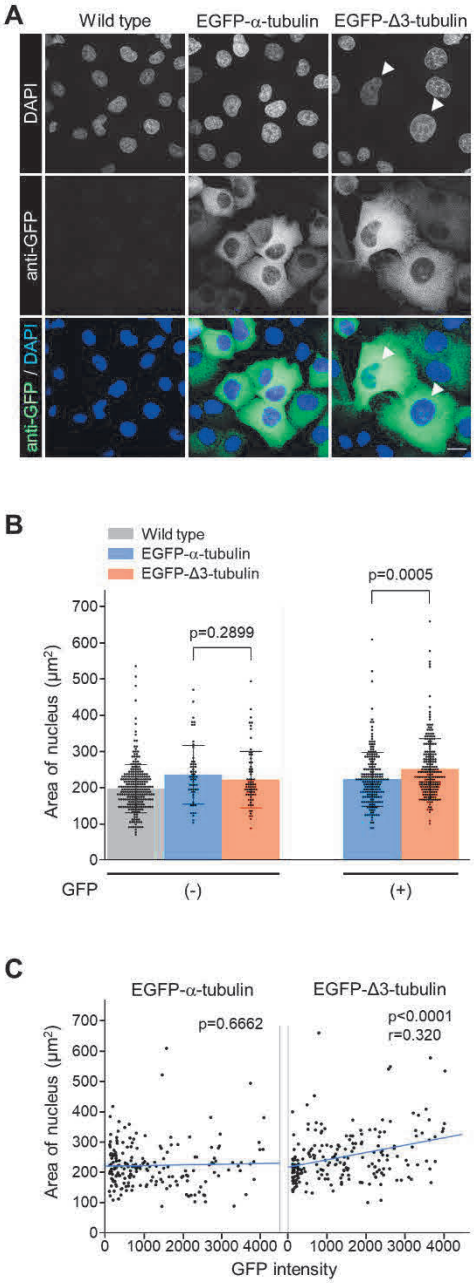
A
Wild type
EGFP-α-tubulin
EGFP-Δ3-tubulin
DAPI
anti-GFP
anti-GFP / DAPI
B
Wild type
EGFP-α-tubulin
EGFP-Δ3-tubulin
p=0.2899
p=0.0005
Area of nucleus (μm²)
GFP
(-)
(+)
C
EGFP-α-tubulin
EGFP-Δ3-tubulin
p=0.6662
p<0.0001
r=0.320
Area of nucleus (μm²)
GFP intensity